THE JOURNAL OF PHYSICAL CHEMISTRY Letters

Letter

Cite This: J. Phys. Chem. Lett. 2018, 9, 281−285

pubs.acs.org/JPCL

# Wannier Koopmans Method Calculations of 2D Material Band Gaps

Mouyi Weng,[†] Sibai Li,[†] Jiaxin Zheng,[†] Feng Pan,[*,†] and Lin-Wang Wang[*,‡]

[†]School of Advanced Materials, Peking University, Shenzhen Graduate School, Shenzhen 518055, People's Republic of China

[‡]Materials Science Division, Lawrence Berkeley National Laboratory, Berkeley, California 94720, United States

Supporting Information

**ABSTRACT:** A major drawback of the widely successful density functional theory is its underestimation of the material band gap. Various methods have been proposed to correct its band gap predictions. Wannier Koopmans method (WKM) is recently developed for this purpose to predict the band gap of extended 3D bulk systems. While the WKM has also been shown to be successful for isolated molecules, it is still a question whether it will work for 2D materials that are in between the 0D molecules and 3D bulk systems. We apply the WKM to 16 commonly known well studied 2D materials and find that the WKM predicted band gaps are on par with their GW calculated results.

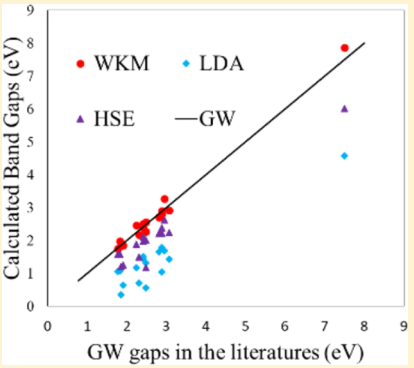




Two-dimensional materials are intensely studied systems in recent years with potentially broad range of applications.[1,2] Because of their unique properties in both the atomic structures and electronic properties, the 2D materials have been used in transistors,[3,4] lithium-ion batteries,[5] metal-air batteries,[6] supercapacitors,[7,8] and solar cell devices.[9] To theoretically study such materials, one basic capability is to predict their fundamental band gaps. This is particularly important for the 2D materials. Because of the insufficient screening, the exciton binding energy is often very large (could be close to 1 eV), and thus the optical absorption spectrum can often not be used to measure the fundamental band gap. Here, by fundamental band gap, we mean the difference between the ionization energy (IE) and electron affinity (EA). Unfortunately, the widely use density functional theory (DFT) often significantly underestimates this fundamental band gap. As a result, the band gap prediction is often done with GW method.[10] The GW calculation of 2D material can be challenging by itself due to difficult *k*-point and number of conduction bands convergence.[11] It is thus helpful if there are alternative methods to calculate the band gaps of such systems.

It is well known that the DFT in either the local density approximation (LDA)[12] or generalized gradient approximation (GGA)[13] significantly underestimates the band gaps, including the 2D material band gaps. There are empirical meta-GGA[13] methods that are proposed to yield better band gaps. There are also hybrid functionals like HSE06, B3LYP[14,15] methods that mix part of the exchange integral in the energy functional. Most of these methods are in a sense empirical in nature, while they work well for the systems included in the original fitting, but they could have significant error for new type of systems. For example, as we have shown before, the HSE06 with the original parameters significantly underestimate the band gaps of alkali halides.[16]

Recently, we have developed a Wannier Koopmans Method (WKM) to calculate the band gaps for bulk materials.[17] This method extends the ΔDFT[18] method that works only for isolated molecules. Traditionally, in ΔDFT method, one calculates EA and IE explicitly using $E(N+1) - E(N)$ and $E(N) - E(N-1)$, respectively, using self-consistent total energy calculations. While the ΔDFT works amazingly well for atoms and small isolate molecules,[18] it fails for extended systems, in which according to Janak's theory[18] the total energy differences just equal the Kohn−Sham eigenenergies. The WKM method solves this problem by placing the extra electron (or the hole) not in the extended Kohn−Sham eigenstates but instead in the localized Wannier functions, meanwhile requiring the satisfaction of Koopmans' theory. This means the total energy as a function of the Wannier function occupation $s_w$ must be linear. To satisfy this Koopmans theory requirement, one additional term is added to the Kohn−Sham Hamiltonian. This term corrects the eigenenergy of the Kohn−Sham equation. More explicitly, we can write down the total energy of the WKM method as

$$E_{\mathrm{WKM}} = E_{\mathrm{LDA}}(\{s_w\}) + \sum_w E_w(s_w)$$

Here the subscribed $w$ indicates different orthogonal Wannier functions and $0 < s_w < 1$ is the occupation number of the Wannier functions $w$. $s_w = 0$ means this Wannier function is not occupied, and $s_w = 1$ means fully occupied Wannier function. For a system with neutral charge, $s_w = 1$ for all Wannier functions constructed from valence band and $s_w =$

**Received:** November 15, 2017
**Accepted:** December 29, 2017
**Published:** December 29, 2017




DOI: 10.1021/acs.jpclett.7b03041
J. Phys. Chem. Lett. 2018, 9, 281−285

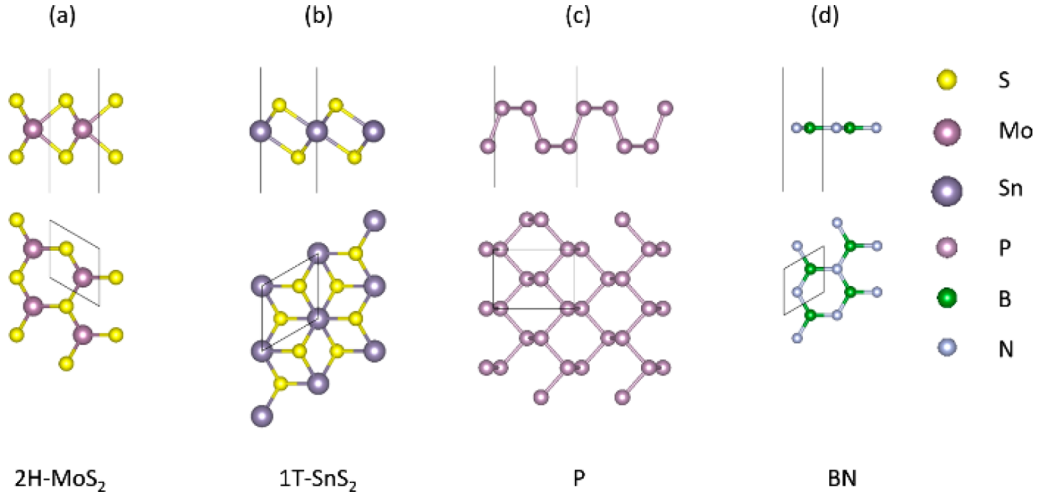


**Figure 1.** Four types of structures used in WKM calculation. (a) 2H type $MX_2$ 2D materials, (b) 1T type MX2 2D materials, (c) black phosphors type 2D materials, and (d) BN type 2D materials.

0 for all of the conduction band Wannier function. $E_{LDA}(\{s_w\})$ is the LDA energy under the condition that Wannier function $w$ is occupied with $s_w$ (see ref 17 for how to calculate $E_{LDA}(\{s_w\})$). To make $E_{WKM}$ linear with $s_w$ for a particular $w$ (starting from the neutral system ground state), the term $E_w(s_w)$ can be expressed as

$$E_w(s_w) = \lambda_w s_w(1 - s_w)$$

The $\lambda_w$ can be obtained from the self-consistent calculation of $E_{LDA}(\{s_w\})$ for a supercell much like for a charged defect calculation. After the Wannier function and the $\lambda_w$ are obtained, a corresponding modified Kohn−Sham equation can be derived by taking the derivative of $E_{WKM}$ with regard to the orbital $\psi_i$, while $s_w = \sum_i \langle w|\psi_i\rangle^2\ o(i)$, where $w$ is the Wannier function and $o(i)$ is the occupation of the Kohn−Sham orbital $\psi_i$. Then the band energy is obtained from the eigenenergy of the modified Kohn−Sham orbital. For details of the calculation, we refer to ref 17.

We have applied the above WKM to 27 common covalent bond semiconductors and all 20 alkali halides.[16,17] This covers the range from covalent bonded semiconductor to the extreme ionic systems. The band gaps of all of these systems agree well with both the experimental results and the GW calculations. The typical error is within a few tenths of an electronvolts for large band gap systems and one or two tenths of an electronvolt for systems with band gaps around 1 to 2 eV. Overall, the band gap error is similar to that of the GW method. We have also tested band alignment between the organic molecular and Au substrate[19] using WKM. The results also agree well with the experiment. At this point, it is important to apply WKM to other types of systems to check its limitation and accuracy.

In the current work, we apply WKM to 16 commonly known 2D materials in their monolayer phases. This is an important test. Because the WKM has been tested for 3D systems and also shown to be accurate for 0D isolated molecules, it is natural to ask what the case is for systems in between. As we discussed in ref 17, the band gap correction of WKM is very much related to the self-interaction correction (SIC) of the LDA Hamiltonian, such SIC should be very different in 2D, 3D, and 0D due to the different screening dimensionality. Unfortunately, not all of the experimental fundamental band gap results are known for 2D materials. For most systems, only the optical band gaps have been measured. As has been shown,[20] the optical band gap can be rather different from the IE-EA fundamental band gap due to the large exciton binding energies for these 2D materials. Because of this, we have compared our results with the GW calculated results for comparison, although there could be some variations in the GW results themselves due to input DFT dependence, $k$-point, and number of conduction band convergence issues. It is particularly challenging to yield converged GW results for these systems.[11,21] Thus, instead of calculating them ourselves, we largely rely on published literatures for GW values. As shown in the Supporting Information, most of the GW results we used are $G_0W_0$ results, while a few are $GW_0$ results when they are available. In our calculation, spin orbital coupling was taken into account. We will also discuss the supercell convergence issue of WKM calculation as well as the Wannier function generations.

Four types of 2D structures are considered, as shown in Figure 1. They are $MX_2$ materials in 2H phase (Figure 1a), $MX_2$ in 2T phase (Figure 1b), black-phosphor-like (or say SnS) 2D materials (Figure 1c), and graphene (or say BN) like 2D materials (Figure 1d). More specifically, we have $MoS_2$, $MoSe_2$, $MoTe_2$, $WS_2$, $WSe_2$ and $WTe_2$ in the 2H phase of Figure 1a and $SnS_2$, $SnSe_2$, $ZrS_2$, $ZrSe_2$, $PtS_2$, and $PtSe_2$ in the 1T phase of Figure 1b. SnS and SnSe have similar structures like black phosphors in Figure 1c (although with two atom types), and we have also calculated the band gap of BN in Figure 1d. All of the lattice constants and positions of atoms can be found in the Supporting Information. We have used the experimental lattice constant from the materials project.[22]

In our calculation, the DFT method was implemented in PWmat code,[23,24] which runs on graphics processing unit (GPU) processors. NCPP-SG15-PBE pseudopotential was used in the calculation.[25,26] For all of the initial LDA calculations (system with two, three, or four atoms unit cells), a 24 × 24 × 1 Monkhorst−Pack k-point set was used to generate Wannier functions.[27] 30 Å is used in the $z$-direction for the bulk calculation to avoid the image interaction. For the calculation in lambda, $k$-point sets vary from different supercell and atom number. Spin−orbital coupling (SOC) is calculated


DOI: 10.1021/acs.jpclett.7b03041
J. Phys. Chem. Lett. 2018, 9, 281−285

with SOC pseudopotential in the NCPP-SG15-PBE format. 60 Ryd plane-wave cutoff is used throughout the calculations.

In our WKM calculations, we first generate Wannier functions by using the Wannier90 code.[28] This, however, is not so straightforward. To get good WKM result, we need localized Wannier functions. Although the final band gap does not sensitively depend on the exact nature of the Wannier functions as long as they are localized, if the generated Wannier function is rather delocalized, then the result can have significant error. To generate localized Wannier functions for the 2D systems, we have the following observations: (a) Try to use as small a number of Wannier functions as possible to represent valence band maximum (VBM) and conduction band minimum (CBM) states. This can minimize the errors from the Wannier90 code. (b) Try to use big enough supercell during the calculation so the Wannier function can be sufficiently localized. Our calculation of $E_{LDA}(\{s_w\})$ is done using a supercell. This is rather like the calculation of a defect state with a charged impurity.

Care must be taken to ensure the convergence of the supercell size to avoid the artificial Coulomb interactions between the image charges. This is particularly intriguing for 2D systems. For example, if the $x$, $y$ directions are fixed, while one increases the $z$-direction supercell size (the distance between two repeating layers), the artificial Coulomb interaction between image charges actually increases linearly with the $z$-direction distance (using a uniform back ground charge to make the whole supercell charge neutral). This is because in an average sense the 2-D plane will have a constant charge planar density and hence a constant electric field perpendicular to the plane, and thus the interaction energy increases linearly to the plane−plane distance. On the contrary, if the distance between the two planes (the $z$-direction supercell size) is fixed, while one increases the $x,y$ direction supercell size $R$, the interaction energy will scale as $\ln(R)$; see the Supporting Information for the derivation. The correct way is to increase all three dimensions on the same scale; in that case, the artificial Coulomb interaction will scale as $1/R$. Thus we could not have a converged lambda if we simply increased the thickness of vacuum layer or increased the $x,y$ dimensions of the supercell while keeping the layer−layer distance unchanged.

As an example, the $p_z$ orbital Wannier function of N atom in the BN valence band is shown in Figure 2a. Its accumulated charge from the center, $Q(r) = \int_{|r'|<r} w(r')d^3r'$, is plotted in Figure 2b for a 9 × 9 × 9 unit super cell. (Here the $z$-direction size, the third 9, is proportionally chosen from the $x,y$ direction size.) We can see that the charge is localized within about 3 Å. The $\lambda_w$ for this particular Wannier function is 2.27 eV when 9 × 9 × 9 supercell is used. It increases to 2.30 eV when a 4 × 4 × 4 supercell is used. However, for a 3 × 3 × 3 supercell, the $\lambda_w$ value increases to 2.97 eV. The convergence of $\lambda_w$ as a function of supercell size is plotted in Figure 3. Similar convergence is found for other Wannier functions and systems. On the basis of this test, in the following calculations of all of the other systems, to have a safe margin, we have used 6 × 6 × 6 supercells to carry out the calculations of $E_{LDA}(\{s_w\})$ to obtain $\lambda_w$.

Our final WKM calculated band gaps (with spin−orbit coupling correction included) are plotted in Figure 4 in comparison with the $G_0W_0$ band gap. The original data can be found in Table S1. We find out that the WKM band gaps are mostly within 0.2 eV of the $G_0W_0$ results. However, there can

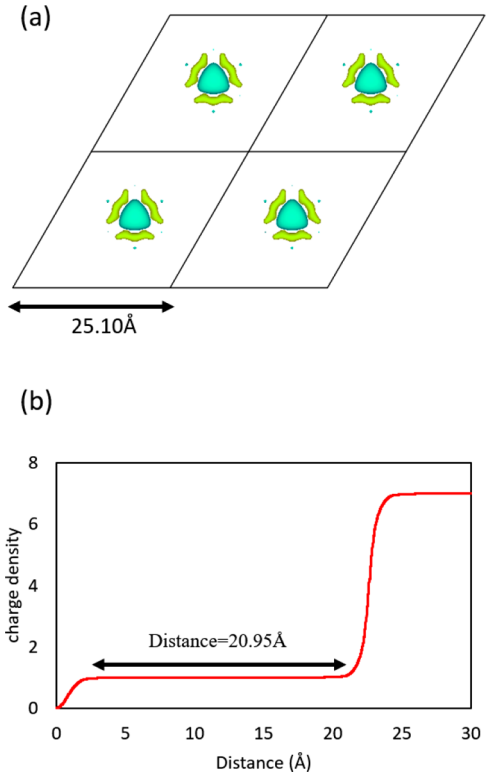


**Figure 2.** (a) Wannier function of pz orbital for N atom in BN valence band. (b) Charge density by the distance from the central of Wannier functions in a supercell of 9.

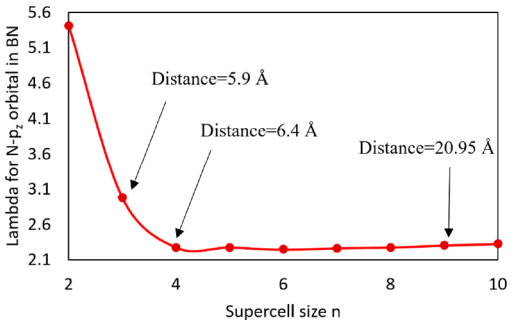


**Figure 3.** BN valence band correction by the supercell used in lambda calculation. The super cell size is $n \times n \times n$; here $n \times n$ is the $xy$ plane supercell in terms of primary cell and $c$ is a dimension in the $z$ direction with its length similar to the primary cell edge length.

be considerable scatter in the literature for the G0W0 band gap for a given 2D materials, as shown in Table S1. For example, monolayer MoS2 has $G_0W_0$ band gap values from 2.67 to 2.84 eV based on different literatures.[11,29−32] Because more conduction bands in the $G_0W_0$ calculation usually result in larger band gaps,[21] we have used the largest $G_0W_0$ results in Table S1 in plotting Figure 4. Overall, we find the agreement between the GW result and the WKM results rather satisfactory, especially given the uncertainties of the GW calculations themselves. We do notice that it is particularly challenging to include a sufficient number of conduction bands in the 2D material GW calculations due to the unbounded nature (extended to the vacuum space) of high-energy conduction bands.

We have also included the LDA band gap and HSE band gap in Figure 4. We see how the WKM significantly improves the



DOI: 10.1021/acs.jpclett.7b03041
J. Phys. Chem. Lett. 2018, 9, 281−285

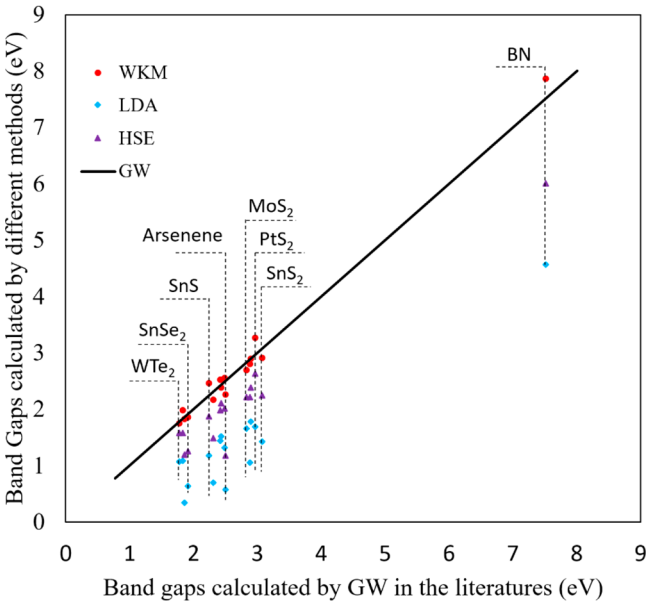


**Figure 4.** Calculated WKM band gap, LDA band gap, and HSE06 band gap versus GW band gaps. Note, for one 2D material, that more than one GW band gap value may be found. We chose the value based on the following decision: If there are both $G_0W_0$ and $GW_0$ calculations, then the self-consistent $GW_0$ values will be used. If there are several $GW_0$ (or several $G_0W_0$ when there is no $GW_0$ calculations), then the one with the largest band gap is used because premature truncation in the number of virtual conduction band can often lead to underestimation of the band gap.

LDA band gap error. To a limited extent, HSE can improve the band gap calculations, but on average it predicts smaller band gaps than $G_0W_0$ band gaps. One can, of course, increase the mixing parameter to increase the band gap in HSE calculation; nevertheless, that can make its prediction of other materials less satisfactory. Thus it is challenging to have a universal set of HSE parameters to reproduce the hand gaps of all materials.

In conclusion, we have applied our WKM method to 2D semiconductors and discussed the procedure to generate the Wannier functions and make the supercell calculations converge. We found that the WKM method predicts the fundamental gap on par with the $G_0W_0$ calculations. This demonstrates once again that the WKM is a rather general method without parameter fitting.

## ■ ASSOCIATED CONTENT

### Supporting Information

The Supporting Information is available free of charge on the ACS Publications website at DOI: 10.1021/acs.jpclett.7b03041.

Details of WKM calculations. (PDF)

## ■ AUTHOR INFORMATION


### Corresponding Authors

*L.-W.W.: E-mail: lwwang@lbl.gov.

*F.P.: E-mail: panfeng@pkusz.edu.cn.

### ORCID

Sibai Li: 0000-0002-4301-132X

Feng Pan: 0000-0002-8216-1339


### Notes

The authors declare no competing financial interest.

## ■ ACKNOWLEDGMENTS

L.-W.W. is supported by the Director, Office of Science (SC), Basic Energy Science (BES), Materials Science and Engineering Division (MSED) of the U.S. Department of Energy (DOE) under Contract No. DE-AC02-05CH11231 through the Materials Theory program (KC2301). This work is also financially supported by National Materials Genome Project of China (2016YFB0700600) and Shenzhen Science and Technology Research Grant (Nos. JCYJ20160226105838578 and JCYJ20151015162256516).

## ■ REFERENCES


(1) Xu, M.; Liang, T.; Shi, M.; Chen, H. Graphene-Like Two-Dimensional Materials. *Chem. Rev.* **2013**, *113*, 3766−3798.

(2) Butler, S. Z.; Hollen, S. M.; Cao, L.; Cui, Y.; Gupta, J. A.; Gutierrez, H. R.; Heinz, T. F.; Hong, S. S.; Huang, J.; Ismach, A. F.; et al. Progress, Challenges, and Opportunities in Two-Dimensional Materials Beyond Graphene. *ACS Nano* **2013**, *7*, 2898−2926.

(3) Wang, Y.; Ye, M.; Weng, M.; Li, J.; Zhang, X.; Zhang, H.; Guo, Y.; Pan, Y.; Xiao, L.; Liu, J.; et al. Electrical Contacts in Monolayer Arsenene Devices. *ACS Appl. Mater. Interfaces* **2017**, *9*, 29273−29284.

(4) Pan, Y.; Li, S.; Ye, M.; Quhe, R.; Song, Z.; Wang, Y.; Zheng, J.; Pan, F.; Guo, W.; Yang, J.; et al. Interfacial Properties of Monolayer MoSe2-Metal Contacts. *J. Phys. Chem. C* **2016**, *120*, 13063−13070.

(5) Tian, L. L.; Li, S. B.; Zhang, M. J.; Li, S. K.; Lin, L. P.; Zheng, J. X.; Zhuang, Q. C.; Amine, K.; Pan, F. Cascading Boost Effect on the Capacity of Nitrogen-Doped Graphene Sheets for Li- and Na-Ion Batteries. *ACS Appl. Mater. Interfaces* **2016**, *8*, 26722−26729.

(6) Tian, L. L.; Yang, J.; Weng, M. Y.; Tan, R.; Zheng, J. X.; Chen, H. B.; Zhuang, Q. C.; Dai, L. M.; Pan, F. Fast Diffusion of O2 on Nitrogen-Doped Graphene to Enhance Oxygen Reduction and Its Application for High-Rate Zn-Air Batteries. *ACS Appl. Mater. Interfaces* **2017**, *9*, 7125−7130.

(7) Peng, L.; Peng, X.; Liu, B.; Wu, C.; Xie, Y.; Yu, G. Ultrathin Two-Dimensional MnO2/Graphene Hybrid Nanostructures for High-Performance, Flexible Planar Supercapacitors. *Nano Lett.* **2013**, *13*, 2151−2157.

(8) Huang, Y.; Zhao, Y.; Gong, Q.; Weng, M.; Bai, J.; Liu, X.; Jiang, Y.; Wang, J.; Wang, D.; Shao, Y.; et al. Experimental and Correlative Analyses of the Ageing Mechanism of Activated Carbon Based Supercapacitor. *Electrochim. Acta* **2017**, *228*, 214−225.

(9) Zeng, H.; Dai, J.; Yao, W.; Xiao, D.; Cui, X. Valley Polarization in MoS2Monolayers by Optical Pumping. *Nat. Nanotechnol.* **2012**, *7*, 490−493.

(10) Hybertsen, M. S.; Louie, S. G. First-Principles Theory of Quasiparticles: Calculation of Band Gaps in Semiconductors and Insulators. *Phys. Rev. Lett.* **1985**, *55*, 1418−1421.

(11) Qiu, D. Y.; da Jornada, F. H.; Louie, S. G. Optical Spectrum of MoS2: Many-Body Effects and Diversity of Exciton States. *Phys. Rev. Lett.* **2013**, *111*, 216805.

(12) Kohn, W.; Sham, L. J. Self-Consistent Equations Including Exchange and Correlation Effects. *Phys. Rev.* **1965**, *140*, A1133−A1138.

(13) Kresse, G.; Furthmüller, J. Efficiency of Ab-Initio Total Energy Calculations for Metals and Semiconductors Using a Plane-Wave Basis Set. *Comput. Mater. Sci.* **1996**, *6*, 15−50.

(14) Stephens, P. J.; Devlin, F. J.; Chabalowski, C. F.; Frisch, M. J. Ab Initio Calculation of Vibrational Absorption and Circular Dichroism Spectra Using Density Functional Force Fields. *J. Phys. Chem.* **1994**, *98*, 11623−11627.

(15) Kim, K.; Jordan, K. D. Comparison of Density Functional and MP2 Calculations on the Water Monomer and Dimer. *J. Phys. Chem.* **1994**, *98*, 10089−10094.

(16) Weng, M.; Li, S.; Ma, J.; Zheng, J.; Pan, F.; Wang, L.-W. Wannier Koopman Method Calculations of the Band Gaps of Alkali Halides. *Appl. Phys. Lett.* **2017**, *111*, 054101.




DOI: 10.1021/acs.jpclett.7b03041
J. Phys. Chem. Lett. 2018, 9, 281−285

(17) Ma, J.; Wang, L.-W. Using Wannier Functions to Improve Solid Band Gap Predictions in Density Functional Theory. *Sci. Rep.* **2016**, *6*, 24924.
(18) Zhan, C.-G.; Nichols, J. a.; Dixon, D. a. Ionization Potential, Electron Affinity, Electronegativity, Hardness, and Electron Excitation Energy: Molecular Properties from Density Functional Theory Orbital Energies. *J. Phys. Chem. A* **2003**, *107*, 4184−4195.
(19) Ma, J.; Liu, Z. F.; Neaton, J. B.; Wang, L.-W. The Energy Level Alignment at Metal-Molecule Interfaces Using Wannier-Koopmans Method. *Appl. Phys. Lett.* **2016**, *108*, 262104.
(20) Zhong, H.; Quhe, R.; Wang, Y.; Ni, Z.; Ye, M.; Song, Z.; Pan, Y.; Yang, J.; Yang, L.; Lei, M.; et al. Interfacial Properties of Monolayer and Bilayer MoS2 Contacts with Metals: Beyond the Energy Band Calculations. *Sci. Rep.* **2016**, *6*, 21786.
(21) Cao, H.; Yu, Z.; Lu, P.; Wang, L.-W. Fully Converged Plane-Wave-Based Self-Consistent GW Calculations of Periodic Solids. *Phys. Rev. B: Condens. Matter Mater. Phys.* **2017**, *95*, 35139.
(22) Jain, A.; Ong, S. P.; Hautier, G.; Chen, W.; Richards, W. D.; Dacek, S.; Cholia, S.; Gunter, D.; Skinner, D.; Ceder, G.; et al. Commentary: The Materials Project: A Materials Genome Approach to Accelerating Materials Innovation. *APL Mater.* **2013**, *1*, 011002.
(23) Jia, W.; Cao, Z.; Wang, L.; Fu, J.; Chi, X.; Gao, W.; Wang, L. W. The Analysis of a Plane Wave Pseudopotential Density Functional Theory Code on a GPU Machine. *Comput. Phys. Commun.* **2013**, *184*, 9−18.
(24) Jia, W.; Fu, J.; Cao, Z.; Wang, L.; Chi, X.; Gao, W.; Wang, L. W. Fast Plane Wave Density Functional Theory Molecular Dynamics Calculations on Multi-GPU Machines. *J. Comput. Phys.* **2013**, *251*, 102−115.
(25) Hamann, D. R. Optimized Norm-Conserving Vanderbilt Pseudopotentials. *Phys. Rev. B: Condens. Matter Mater. Phys.* **2013**, *88*, 085117.
(26) Schlipf, M.; Gygi, F. Optimization Algorithm for the Generation of ONCV Pseudopotentials. *Comput. Phys. Commun.* **2015**, *196*, 36−44.
(27) Pack, J. D.; Monkhorst, H. J. Special Points for Brillouin-Zone Integrations. *Phys. Rev. B* **1976**, *13*, 5188−5192.
(28) Souza, I.; Marzari, N.; Vanderbilt, D. Maximally Localized Wannier Functions for Entangled Energy Bands. *Phys. Rev. B: Condens. Matter Mater. Phys.* **2001**, *65*, 35109.
(29) Rasmussen, F. A.; Thygesen, K. S. Computational 2D Materials Database: Electronic Structure of Transition-Metal Dichalcogenides and Oxides. *J. Phys. Chem. C* **2015**, *119*, 13169−13183.
(30) Liang, Y.; Huang, S.; Soklaski, R.; Yang, L. Quasiparticle Band-Edge Energy and Band Offsets of Monolayer of Molybdenum and Tungsten Chalcogenides. *Appl. Phys. Lett.* **2013**, *103*, 042106.
(31) Qiu, D. Y.; da Jornada, F. H.; Louie, S. G. Screening and Many-Body Effects in Two-Dimensional Crystals: Monolayer MoS2. *Phys. Rev. B: Condens. Matter Mater. Phys.* **2016**, *93*, 235435.
(32) Ramasubramaniam, A. Large Excitonic Effects in Monolayers of Molybdenum and Tungsten Dichalcogenides. *Phys. Rev. B: Condens. Matter Mater. Phys.* **2012**, *86*, 115409.



DOI: 10.1021/acs.jpclett.7b03041
*J. Phys. Chem. Lett.* 2018, 9, 281−285